

NASA Technical Memorandum 100213  
AIAA-88-0131

# A Natural Low Frequency Oscillation in the Wake of an Airfoil Near Stalling Conditions

{NASA-TM-100213} A NATURAL LOW FREQUENCY  
OSCILLATION IN THE WAKE OF AN AIRFOIL NEAR  
STALLING CONDITIONS {NASA} 17 p Avail:  
NTIS HC A03/MF A01 CSCL 01A

N88-10779

G3/02 Unclas  
0106498

K.B.M.Q. Zaman and D.J. McKinzie  
*Lewis Research Center*  
*Cleveland, Ohio*

Prepared for the  
26th Aerospace Sciences Meeting  
sponsored by the American Institute of Aeronautics and Astronautics  
Reno, Nevada, January 11-14, 1988



# A NATURAL LOW FREQUENCY OSCILLATION IN THE WAKE OF AN AIRFOIL NEAR STALLING CONDITIONS

by

K.B.M.Q. Zaman and D.J. McKinzie  
National Aeronautics and Space Administration  
Lewis Research Center  
Cleveland, Ohio 44135

## Abstract

An unusually low frequency oscillation in the flow over an airfoil was explored experimentally. Wind tunnel measurements were carried out with a two-dimensional airfoil model at a chord Reynolds number of  $10^5$ . During deep stall, at  $\alpha > 16^\circ$ , the usual "bluff-body shedding" occurred at a Strouhal number,  $St_s = 0.2$ . But at the onset of stall around  $\alpha = 15^\circ$ , a low frequency periodic oscillation occurred, the corresponding  $St_s$  being an order of magnitude lower. The phenomenon took place in relatively "unclean" flow when the freestream turbulence was raised to 0.4 percent, but did not in the cleaner flow with turbulence intensity of 0.1 percent. It could also be produced by certain high frequency acoustic excitation. Details of the flow field are compared between a case of low frequency oscillation at  $\alpha = 15^\circ$  and a case of bluff-body shedding at  $\alpha = 22.5^\circ$ . The origin of the low frequency oscillation traces to the upper surface of the airfoil and is seemingly associated with the periodic formation and breakdown of a large separation bubble. The intense flow fluctuations impart significant unsteady forces to the airfoil but diminish rapidly within a distance of one chord from the trailing edge. At the latter downstream location, the periodic concentration of the spanwise component of vorticity is found to be much lower in the low frequency case than that in the bluff body shedding case.

## Nomenclature

$c$	airfoil chord
$f_p$	acoustic excitation frequency
$f_s$	shedding frequency
$Re$	chord Reynolds number, $U_\infty c/\nu$
$St_p$	$f_p c/U_\infty$
$St_s$	$f_s c \sin \alpha/U_\infty$
$u'_f$	fundamental r.m.s. velocity fluctuation at frequency $f_s$
$u'(f)$	one-dimensional, longitudinal velocity spectra
$u'_\infty$	freestream, r.m.s., longitudinal velocity fluctuation
$U_\infty$	freestream mean velocity
$\alpha$	angle of attack
$\nu$	kinematic viscosity

## 1. Introduction

The low frequency oscillation of flow over an airfoil, studied in this paper, was observed earlier at NASA Langley by Zaman et al.<sup>1</sup> This observation was based on velocity spectra measurements in the airfoil wake, around static stall condition. The spectra exhibited a sharp spike at an unusually low frequency which varied continuously with the freestream speed. The frequency was low with a corresponding Strouhal number ( $St_s$ ) of only about 0.02, as compared to order(s) of magnitude higher values observed previously in cases involving bluff-body shedding,<sup>2</sup> trailing edge noise,<sup>3</sup> etc. The present experiment was an attempt to obtain a better understanding of the phenomenon.

However, the phenomenon could not be reproduced in the initial attempt in a relatively cleaner wind tunnel at NASA Lewis. Later on, it could be when either the tunnel freestream turbulence was raised artificially or the flow was excited acoustically at some high frequencies. The present paper describes essential data illustrating these effects together with some details of the unsteady flow field associated with the low frequency oscillation. As this is essentially a status report, discussions on the significance of the results is deferred to the end of the paper. In section 4, the inferences made so far are first summarized. This is followed by a brief literature review including recent observations in the cylinder wake. Also discussed are possible connection of the phenomenon to stall flutter, a parallel computational study on airfoils encountering similar low frequency flow oscillation, and our future plans.

## 2. Experimental Facility

The experiments were carried out in a low speed wind tunnel having a test section with 76 by 51 cm cross section. The flow entered through a 16:1 contraction section with five screens, passed through the test section and was then exhausted by an axial fan. The freestream turbulence intensity was less than 0.1 percent, but could be increased by installing turbulence generating screens 37 cm upstream from the airfoil support. The two-dimensional airfoil model, with 12.7 cm chord, was of the same cross-sectional shape as in the Langley experiment (LRN(1)-1007); however, the aspect ratio was 6:1 as opposed to 3:1 at Langley. It was supported rigidly, on the two ends, both in torsion and lateral movements. However, whenever the low frequency shedding occurred, the airfoil vibrated perceptibly, at the same frequency, the midspan section going through a displacement of about 1 mm. Lift and drag could be measured by loosening the airfoil mount on to a balance mechanism. There was provision for acoustic excitation through a loud

speaker mounted on the ceiling of the test section. Velocity measurements were made by standard hot-wire anemometry.

Most data reported are for  $Re = 10^5$ . A schematic of probe arrangement, used for conditional sampling measurements, to be elaborated later, is shown in Fig. 1. The X-wire probe could be traversed in the streamwise direction ( $x$ ) through a longitudinal slot on the floor of the test section. For a given  $x$ , the entire slot was sealed; in this position, the probe could be moved up and down (in  $y$ ) through automated computer control without disturbing the seal. The co-ordinate origin is at the airfoil support at one quarter chord from the leading edge;  $z = 0$  corresponds to the midspan.

### 3. Results

Figure 2 shows  $u'$ -spectra measured with a fixed single hot-wire about one chord downstream of the airfoil trailing edge. The freestream turbulence was raised to about 0.4 percent for these data. The spectra traces are staggered and are for different  $\alpha$  as indicated. At  $\alpha = 18^\circ$  and  $20^\circ$ , the spectral peaks at the relatively higher frequencies represent the bluff-body shedding and correspond to  $St_S = 0.2$ . At lower angles of attack, the flow is attached and no spectral peaks occur in the frequency range covered. (At certain small angles, however, there were higher frequency spectral peaks, apparently scaling on the airfoil thickness; this aspect will not be pursued here.) Around  $\alpha = 15^\circ$ , a spectral peak at 7.5 Hz occurs unambiguously. This corresponds to  $St_S = 0.02$ , a value found to remain approximately constant at a few other speeds and agreeing with previous data at Langley.

As indicated before, the occurrence of the low frequency oscillation had been illusive and puzzling. It could not be reproduced in the initial attempt. This can be appreciated from Fig. 3. Spectra traces similar to (a) were obtained at first in which the sharp low frequency peak was absent. Only when the freestream turbulence was increased by the addition of a 30 mesh screen, did it result in the spectral spike as in trace (c). Trace (b) shows that a high frequency acoustic excitation, of the otherwise same flow as in (a), also produced the low frequency oscillation. However, the acoustic excitation at even higher frequencies had an opposite effect of eliminating the low frequency peak otherwise occurring naturally in case (c).

The acoustic excitation effect is illustrated in Fig. 4. The fundamental rms velocity fluctuation at the oscillation frequency (7.5 Hz) is shown as a function of the excitation Strouhal number,  $St_p$ . For each data point the sound pressure level measured by a flush mounted microphone on the ceiling was held constant at 104 dB (re,  $0.00002 \text{ N/m}^2$ ). The two sets of data were obtained successively, keeping all conditions unchanged except for the insertion of the 30 mesh screen. There is no effect in either case at low  $St_p$ . But in the  $St_p$ -range of 20 to 25, the excitation enhances the periodicity in the no-screen case. Note that excitation in a  $f_p$  range of 2 to 2.5 kHz yields an oscillation at 7.5 Hz. At even higher  $f_p$  the broadband energy at 7.5 Hz is diminished. In the flow with the screen, the naturally occurring

spectral peak at 7.5 Hz remains unaffected up to  $St_p = 25$ , but excitation at higher  $St_p$  eliminates the peak. Excitation effect similar to the latter was also observed in the Langley experiment.<sup>1</sup> Note that no screens were used in the Langley experiment but the natural freestream turbulence was higher, about 0.25 percent.

The observed effects of the freestream turbulence and the acoustic excitation on the low frequency oscillation have remained unresolved. Attempts to unravel these effects did not seem prospective at this time. It was felt that a better understanding of the associated unsteady flow field was needed to proceed further. Thus, an effort was made to obtain flow field data for a typical case of the low frequency shedding. For comparison, also obtained were corresponding data for a typical bluff-body shedding case. In the following, comparative data are presented for: (1)  $\alpha = 15^\circ$  yielding a 7.5 Hz shedding and (2)  $\alpha = 22.5^\circ$  yielding a 49 Hz shedding. Case (1) is elaborated more as appropriate. In both cases, the flow was without any acoustic excitation, but the screen was used to raise the freestream turbulence to 0.4 percent; the chord Reynolds number was  $10^5$ .

Figure 5(a) shows the fundamental rms velocity fluctuation amplitudes at the respective frequencies for the two cases as a function of streamwise distance. These measurements were made along the midspan ( $z = 0$ ) at a constant height slightly above the airfoil upper surface ( $y/c = 0.1$ ). It is clear that the low frequency oscillation has very large amplitudes but it decays rapidly with  $x$ . Note that the region of large fluctuation is between 0.25 and 0.5  $c$  from the leading edge. The flow fluctuations exert large unsteady forces on the airfoil. In fact, the airfoil started fluttering as soon as it was loosened from its rigid mount. For the bluff-body shedding case, the amplitude of the spectral peak is small shortly downstream of the trailing edge; over the airfoil the peak was not visible in the spectra.

Figure 5(b) shows the axial variation of the phase corresponding to the data of Fig. 5(a). The slopes of these phase curves, measured in the range  $x/c > 2$ , yielded wavelengths of 8.6 and 1.8  $c$  for the low and the high frequency cases, respectively; the corresponding phase velocities turned out to be  $0.7 U_\infty$  and  $0.94 U_\infty$ , respectively. The phase speed result is proof that the low frequency oscillation is hydrodynamic in nature and not due to, say, a standing acoustic wave.

The transverse variation of the fundamental amplitude and phase, one chord downstream from the trailing edge, at midspan, are shown in Figs. 6(a) and (b). The amplitude for the low frequency case is small all across the wake at this station. The amplitude due to the bluff-body shedding is larger especially on the lower side of the airfoil (at negative  $y$ ). The corresponding variations for the  $\alpha = 15^\circ$  case only, measured over and below the airfoil at 40 percent chord location from the leading edge, are shown in Fig. 7. The  $\alpha = 15^\circ$  case data from Fig. 6 are repeated for easy comparison. The gaps in the dashed curves (Fig. 7) represent regions that could not be accessed by the hot-wire mounted on a horizontal support.

For the  $\alpha = 15^\circ$  case, the amplitude is much more intense over the upper surface of the airfoil

(Fig. 7(a)). The peak occurs about 8.3 mm from the airfoil surface where the local mean velocity is about 90 percent of the freestream velocity. Corresponding mean velocity profile, despite the hot-wire rectification, provided an indication that the separation bubble at this location extended about 6 mm from the surface on a time average basis. Note that on the lower side of the airfoil the amplitude is small. Figure 7(a) together with Fig. 5(a) strongly indicate that the origin of the low frequency oscillation is on the upper surface, near the leading edge, most likely due to the periodic bursting of a separation bubble.

Representative flow visualization pictures for the low frequency oscillation case, obtained with a horizontal smoke wire placed about 5 cm upstream from the airfoil leading edge, are shown in Figs. 8 and 9. These pictures are from movie sequences, but are for a lower freestream velocity ( $R_c = 7.5 \times 10^4$ ) yielding a flow oscillation at 5.5 Hz. Motion pictures were also obtained for  $R_c = 10^5$  but the contrast and the quality of the pictures turned out to be much better at the lower  $R_c$ . From close observation of the movies, the general features of the flow patterns at the two Reynolds numbers were found to be the same.

Each movie sequence captured about one half of a second of smoke streaks from the smoke wire, and thus was expected to contain two or three periods of the low frequency oscillation. However, the phenomenon was not strictly periodic and the "irregularities" and "drop outs" rendered the visualization experiment very difficult. The following inferences are based on inspection of about a dozen similar movie sequences.

The two pictures in Fig. 8 are separated by about 90 ms. This corresponds to a phase difference of about  $180^\circ$ . The top picture shows a relatively more attached flow on the upper surface, while the formation of a large separation bubble is apparent in the lower picture. A periodic up and down "flapping" motion of the layer of smoke streaks on the airfoil upper surface was the most readily and easily discernible flow characteristic in the movies. As far as could be determined, this motion was approximately two-dimensional or uniform in the spanwise direction, except for a small region near the tunnel wall.

Figure 9 shows a closer view of the smoke streaks on the upper surface but at the same time covering the flow field somewhat farther downstream. The time differences, relative to the instant of the top picture, are indicated; note that the times are not equally spaced. The gradual build up and the subsequent collapse of the separation bubble can be easily observed. Another feature which became apparent from this camera angle is the formation of a large "cork-screw-like" structure downstream of the airfoil. This structure, visible in the pictures for 90 and 100 ms (marked by arrows), apparently forms shortly after the separation bubble reaches its largest size and starts to collapse. Viewing from downstream, this structure has a clockwise rotation, and appears similar to a "trailing vortex" (see, e.g., p. 51 of Ref. 4). It is not known at this point whether there is a counterpart vortex on the other end of the airfoil and if it plays a role in sustaining the low frequency oscillation.

Conditionally averaged data are presented in the following for the two flows of Figs. 5 and 6. But first, the nature of the two basic wakes on a time average basis are further documented in Figs. 10(a) to (c). The mean velocity and the longitudinal and transverse turbulence intensity profiles, measured at  $x/c = 1.75$ , are shown. The wider and deeper wake for the  $\alpha = 22.5^\circ$  case (Fig. 10(a)) represents a higher drag, as expected. The turbulence intensities are also higher for the  $22.5^\circ$  case; in both cases the  $v'$ -levels are found to be somewhat higher than the corresponding  $u'$ -levels.

The conditional averaging measurements were carried out with the help of an X-wire and reference probes as shown in Fig. 1. Probes 1 and 2 provided appropriate reference signals. Their locations are shown approximately to scale and were chosen to capture the velocity fluctuations at their strongest amplitudes. Sample reference signals for the low frequency case (probe 1) and the high frequency case (probe 2) are shown in Fig. 1; these have been bandpass filtered in the bands 1 to 20 Hz and 10 to 200 Hz, respectively.

For each  $y$ -location of the X-wire probe, the  $u$ -,  $v$ - and the appropriate reference signal were recorded digitally. The post-processing was similar to that done in Ref. 5. The negative peaks in the reference signals were used as triggers for data sampling. A threshold of  $2\sigma$  was used to discriminate the negative peaks,  $\sigma$  being the standard deviation of the respective reference signal. Centered around the triggers, sample functions consisting of 37 data were accepted for the  $u$ - and the  $v$ -signals. Ensemble averaging was performed assuming a triple decomposition,

$$\tilde{f} = F + f_c + f_r, \text{ yielding,}$$

$$\langle \tilde{f} \rangle = \langle f \rangle = F + \langle f_c \rangle.$$

$F$ ,  $f_c$ , and  $f_r$  are the time-average, the "coherent" and the "incoherent" components of the instantaneous function  $\tilde{f}$ , respectively.

The distributions of  $\langle u \rangle$  and  $\langle v \rangle$  as a function of time ( $\tau$ ) were obtained at different  $y$ . From these the ensemble averaged spanwise vorticity was obtained invoking Taylor hypothesis:<sup>5</sup>

$$\langle \omega_z \rangle = (1/0.7 U_\infty) (d\langle v \rangle / d\tau) - d\langle u \rangle / dy$$

Note that  $\langle \omega_z \rangle$  includes the time-average contribution, and that the convection velocity used in the Taylor hypothesis is  $0.7 U_\infty$  which is approximately representative of both the cases at the measurement location. (Note in Fig. 5(b) that the slope of the phase curve for  $\alpha = 22.5^\circ$  changes, accounting for a different phase velocity at  $x/c = 1.75$  compared to the value  $0.94 U_\infty$  measured downstream.)  $\langle \omega_z \rangle$  distributions, nondimensionalized by  $c/U_\infty$ , for the two cases under consideration are shown in Fig. 11(a) and (b). The abscissae are normalized by the respective periods. The Karman-vortex-street type structure appears in the bluff-body shedding case. There are concentrations of vorticity of opposite sign on the two sides of the wake. Note that the "shedding" frequency corresponds to half the total number of vortices shed from the airfoil. Interestingly, in the low frequency case, except for an undulation with time, the  $\langle \omega_z \rangle$  distribution is

not much different from the two layers of time-average vorticity expected from the  $U(y)$  distribution of Fig. 10(a). The lower concentration of vorticity in this case is consistent with the amplitude data of Fig. 6(b).

#### 4. Discussion

The present paper documents data on an interesting phenomenon of low frequency oscillation of flow over an airfoil that is different in many ways from the relatively well-known bluff-body shedding. As stated earlier, there were puzzling effects of freestream turbulence and acoustic excitation on the phenomenon which have remained unresolved. An attempt was made to obtain an understanding of the unsteady flow-field associated with a typical case. The inferences clearly drawn so far are as follows: (1) the phenomenon is hydrodynamic and not associated with a standing acoustic mode, (2) its origin lies on the upper surface of the airfoil near the leading edge region and is linked to the periodic formation and breakdown of a large separation bubble, and (3) the flow fluctuations are intense over the airfoil but decay rapidly with downstream distance.

Commensurate with the last inference, the vorticity fluctuation, measured one chord downstream of the trailing edge, is found to be small compared to the corresponding data for an example of bluff-body shedding. Whether the (spanwise) vorticity concentration for the low frequency case is also low near and over the airfoil is unclear at this time.

One of the difficulties in the present experiment, especially in the flow visualization, was the very low frequency involved in the phenomenon. The smoke-wire technique employed had typical smoke duration of about one half of a second. Thus, only about three periods of the oscillation were expected to be captured in a sequence of the movies. This was aggravated by the fact that the oscillation was not exactly periodic and involved frequent "dropouts."

The low frequency flow oscillation has been observed to exert large unsteady forces on the airfoil. Thus, the phenomenon could be considered as a probable mechanism for inducing stall flutter. Flutter of wings and blades is the unsteady motion induced by aerodynamic instabilities; when the latter couples with structural instabilities the problem is the most serious. As far as the aerodynamic aspect of it, a review of the literature suggests that stall flutter has been typically associated with bluff-body shedding.<sup>6</sup> However, the flutter boundary data for a NACA 64-012 airfoil, cited in Ref. 6, on a careful examination, is found to extend over the Strouhal number ( $St_S$ ) range of 0.03 to 0.16. While it is possible that the boundary cited in Ref. 6 could be different with other airfoils, it is interesting that the above range extends approximately to the low frequency observed here and terminates somewhat short of the bluff-body shedding frequency.

Limited literature search yielded two other earlier works which reported low frequency vibrations of airfoils at Strouhal numbers close to the present observation. Farren (1935)<sup>7</sup> primarily reported lift and drag data on oscillating airfoils; but he also presented a set of data for a

fixed airfoil (at  $\alpha = 14^\circ$ ) in which the lift varied periodically at a frequency that apparently corresponded to  $St_S = 0.02$ . Reference 8 reported results on acoustic excitation effect on unsteady stall; from normal force fluctuation spectra, large amplitude natural oscillations were reported at around  $St_S = 0.05$ . We expect to carry out a complete literature survey and discuss further on related earlier observations in an upcoming publication. It is worth mentioning that low frequency oscillations have also been observed in various other flows involving separation. These include transitory stall in diffusers, flow behind a step, etc.; Ref. 9 provides a review.

The evolution of the spanwise vorticity in the low frequency oscillation case is to be further explored in an upcoming experiment. Also to be addressed are a host of other questions that arise at this point, including: (1) can the flow oscillation be made periodic by artificial excitation? A periodic motion would render the unsteady measurements (phase-averaging) enormously easier. (2) How does the amplitude and phase vary in the spanwise ( $z$ ) direction? What is the role of the trailing-vortex-like structure in the phenomenon? (3) Does the low frequency oscillation take place with other airfoils of different cross-sectional shape and span? (4) What is the role of possible structural vibrations in the phenomenon?

The last point has become specially crucial in view of a similar but controversial observation in the wake of a circular cylinder. Srineivasan<sup>10</sup> reported experimental observation of a velocity spectral peak in the cylinder wake at a frequency "incommensurately" lower than the expected "Strouhal frequency." Peaks at both frequencies together with several others at the sum and difference frequencies and their harmonics, appeared in the spectra. With increasing Reynolds number, a sequence of transformation took place from "orderliness" to "chaos" and the re-emergence of "orderliness," within the  $Re$ -range of 35 to 170 covered in the experiment. Srineivasan considered these sequences as a precursor to transition, from the perspective of a nonlinear dynamical system. Interestingly, the frequency of the secondary spectral component was often an order of magnitude lower than the Strouhal frequency, akin to the observation in the present airfoil study. However, Van Atta and Gharib<sup>11</sup> in a subsequent experiment, similar to that of,<sup>10</sup> traced the origin of the lower frequencies to cylinder vibration. They observed that, depending on the flow and the cylinder (wire) tension, the spectra contained peaks at the main Strouhal frequency and at a certain (super)harmonic of the fundamental vibration frequency, the difference between the two corresponded to the lower frequency peak. However, the present authors' impression is that the matter is not completely resolved yet, as Srineivasan (private communication), based on a repeated experiment, believes that cylinder vibration is not a necessary condition for the generation of the lower frequency components.

The question naturally arises if airfoil vibration in our experiment resulted in the low frequency oscillation. As mentioned earlier, there was perceptible vibration of the airfoil, and it would be impossible in practice to completely restrain the airfoil. Vibration is to be probed further, but the following should indicate

that the airfoil vibration was a result of the unsteady flow fluctuations and not the vice versa. (1) When the low frequency occurred, there was only one spectral peak at the corresponding frequency. Note that the basis for the explanation in Ref. 11 was the fact that the low frequency was the difference between the Strouhal frequency and a (super)harmonic of the cylinder vibration frequency, spectral peaks appearing clearly at all three. (2) The same low frequency occurred in two different wind tunnels involving a factor of two difference in the airfoil aspect ratio. The vibrational characteristics could be expected to be different in the two experiments. (3) The oscillation appeared or disappeared in the otherwise same flow and structural environment depending on the free-stream turbulence or a high frequency acoustic excitation.

A further indication that the origin of the low frequency shedding lies in the "sensitivity" of the separation bubble comes from a numerical study. Rumsey,<sup>12</sup> in computing the unsteady flow over airfoils, has encountered a rather strikingly similar result as in the present experiment. A two-dimensional algorithm based on the "thin-layer" form of the compressible Navier-Stokes equation yielded a low frequency fluctuation in the flow-field of a NACA-0012 airfoil. The computation carried out for  $\alpha = 18^\circ$  showed that if the boundary layer on the airfoil surface was assumed laminar, the shedding Strouhal number was 0.155, but if it was assumed turbulent the shedding Strouhal number dropped to 0.03. The unsteady forces on the airfoil, as manifested by a variation in the lift coefficient, were found to be much larger in the low frequency case than at the higher one. However, a similar computation for flow over a cylinder by Townsend et al.<sup>13</sup> indicated that apparent low frequency oscillation can result due to reflections from the computational domain boundary. But this is unlikely to be a problem in<sup>12</sup> as nonreflective boundary conditions were ensured (Rumsey, private communication). The latter notion is further supported by the fact that in the same computational domain, the low frequency oscillation appeared when the boundary layer was assumed turbulent and did not when it was assumed laminar. At this point, it is not clear whether the phenomena observed experimentally by us and computationally by Rumsey are the same, but we hope that a joint effort, currently under way, should provide some answers in the near future.

#### References

1. Zaman, K.B.M.Q., Bar-Sever, A., and Mangalam, S.M., "Effect of Acoustic Excitation on the Flow Over a Low-Re Airfoil," Journal of Fluid Mechanics, Vol. 182, Sept. 1987, pp. 127-148.
2. Roshko, A., "On the Drag and Shedding Frequency of Two-Dimensional Bluff Bodies," NACA TN-3169, 1954.
3. Brooks, T.F. and Schlinker, R.H., "Progress in Rotor Broadband Noise Research," Vertica, Vol. 7 No. 4, 1983, pp. 287-307.
4. Van Dyke, M., An Album of Fluid Motion, The Parabolic Press, 1982.
5. Zaman, K.B.M.Q. and Hussain, A.K.M.F., "Taylor Hypothesis and Large-Scale Coherent Structures," Journal of Fluid Mechanics, Vol. 112, Nov. 1981, pp. 379-396.
6. Ericsson, L.E., "Effect of Karman Vortex Shedding on Airfoil Stall Flutter," 4th AIAA Applied Aerodynamics Conference, AIAA, New York, 1986, pp. 162-169.
7. Farren, W.S., "Reaction on a Wing Whose Angle of Incidence is Changing Rapidly. Wind Tunnel Experiments with a Short Period Recording Balance," ARC-R&M No. 1648, Aeronautics Laboratory, Cambridge, Jan. 1935.
8. Moss, N.J., "Measurements of Aerofoil Unsteady Stall Properties with Acoustic Flow Control," Journal of Sound and Vibration, Vol. 65, No. 4, Aug. 22, 1979, pp. 505-520.
9. Simpson, R.L., "Two-Dimensional Turbulent Separated Flow," AGARD-AG-287-VOL-1, June 1985. (Avail. NTIS, AD-A160659.)
10. Sreenivasan, K.R., "Transitional and Turbulent Wakes and Chaotic Dynamical Systems," Nonlinear Dynamics of Transcritical Flows, H.L. Jordan, H. Oertel, and K. Robert, eds., Springer-Verlag, Berlin, 1985, pp. 59-80.
11. Van Atta, C.W. and Gharib, M., "Ordered and Chaotic Vortex Streets Behind Circular Cylinders at Low Reynolds Numbers," Journal of Fluid Mechanics, Vol. 174, Jan. 1987, pp. 113-133.
12. Rumsey, C.L., "A Computational Analysis of Flow Separation Over Five Different Airfoil Geometries at High Angles-of-Attack," AIAA Paper 87-0188, Jan. 1987.
13. Townsend, J.C., Rudy, D.H., and Sirovich, L., "Computation and Analysis of a Cylinder Wake Flow," Forum on Unsteady Flow Separation, ASME FED Vol. 52, ASME, New York, 1987, pp. 165-174.

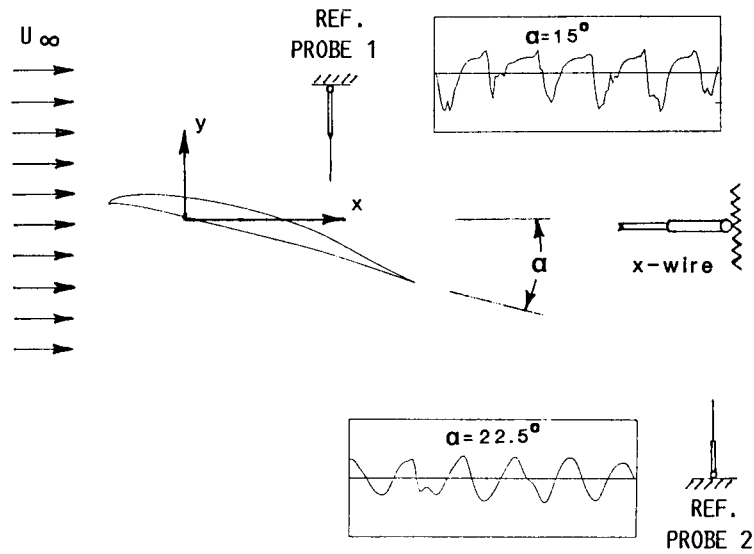


FIGURE 1. - SCHEMATIC OF EXPERIMENTAL SETUP. INSETS ARE FIL-  
TERED  $\tilde{u}$ -SIGNALS FROM THE REFERENCE PROBES AT INDICATED  
ANGLES OF ATTACK ( $\alpha$ ); RECORD LENGTHS ARE 732 MS AND 112 MS  
FOR PROBES 1 AND 2, RESPECTIVELY.

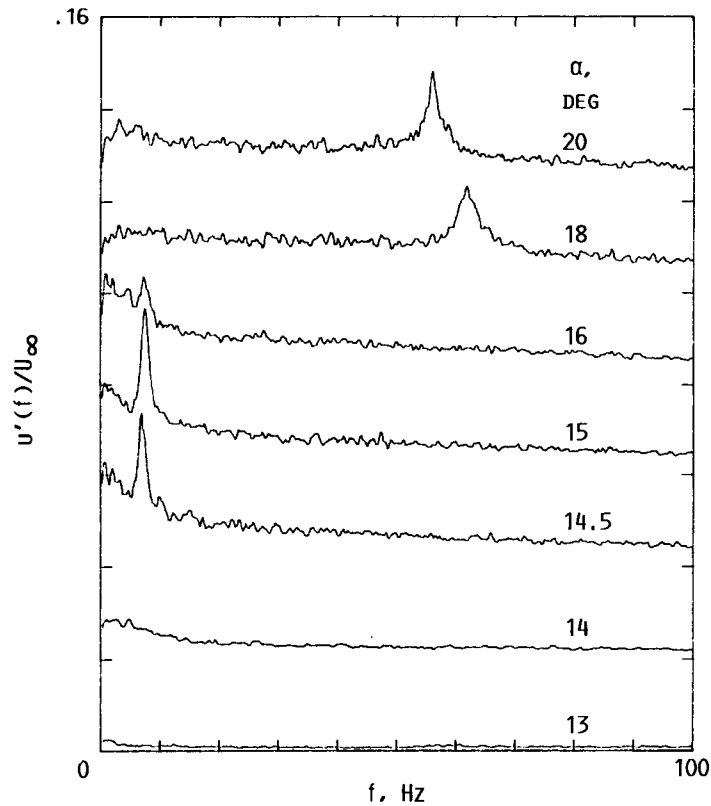


FIGURE 2. -  $u'-(f)$ -SPECTRA MEASURED AT  $x/c = 1.75$ ,  
 $z = 0$ , AND  $y/c = 0.1$ . SPECTRA TRACES ARE  
STAGGERED SUCCESSIVELY BY ONE ORDINATE DIVI-  
SION AND ARE FOR INDICATED  $\alpha$ .  $R_c = 10^5$ ,  
 $u'_\infty/U_\infty = 0.4\%$ .

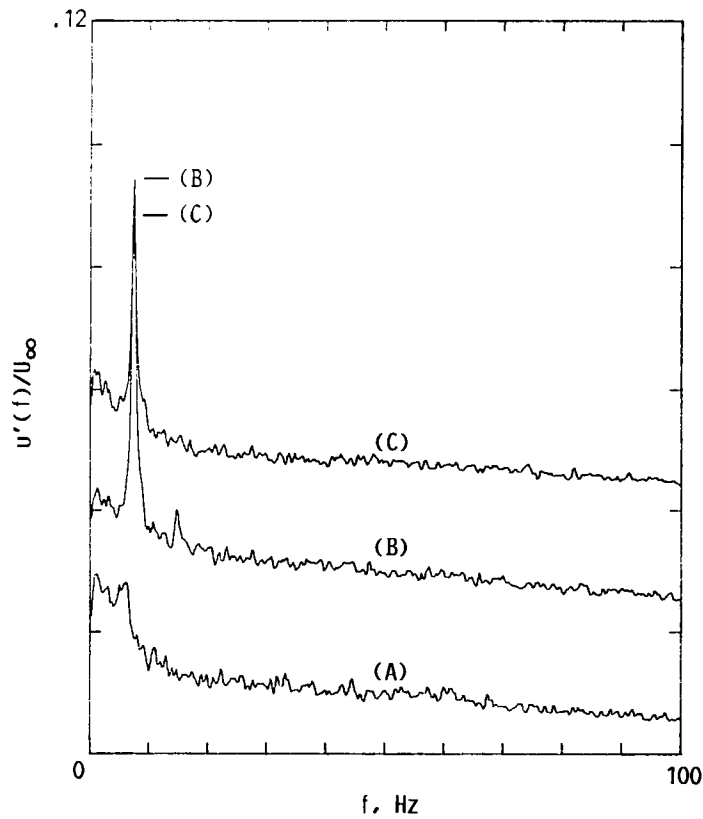


FIGURE 3. -  $u'$ -SPECTRA, MEASURED AT  $x/c = 1.75$ ,  $z = 0$ , AND  $y/c = 0.1$ , AT  $\alpha = 15^\circ$  AND  $R_c = 10^5$ .  
 (A)  $u'_\infty/U_\infty = 0.1\%$ ; (B)  $u'_\infty/U_\infty = 0.1\%$  WITH ACOUSTIC EXCITATION AT 2540 Hz; (C)  $u'_\infty/U_\infty = 0.4\%$ .

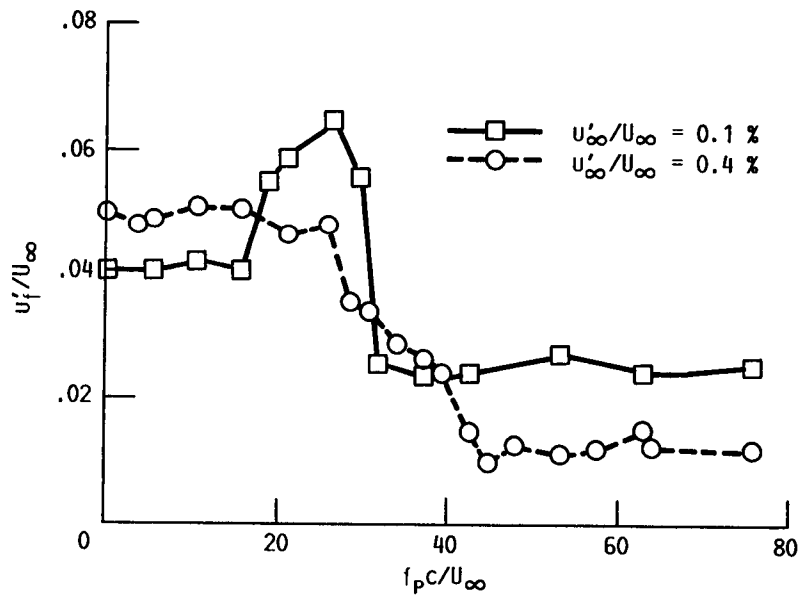


FIGURE 4. - VARIATION OF BAND PASSED ( $\Delta f = 0.25$  Hz) RMS VELOCITY FLUCTUATION, AT 7.5 Hz, WITH EXCITATION STROUHAL NUMBER. MEASUREMENT AT  $x/c = 1.75$ ,  $z = 0$ , AND  $y/c = 0.1$ .



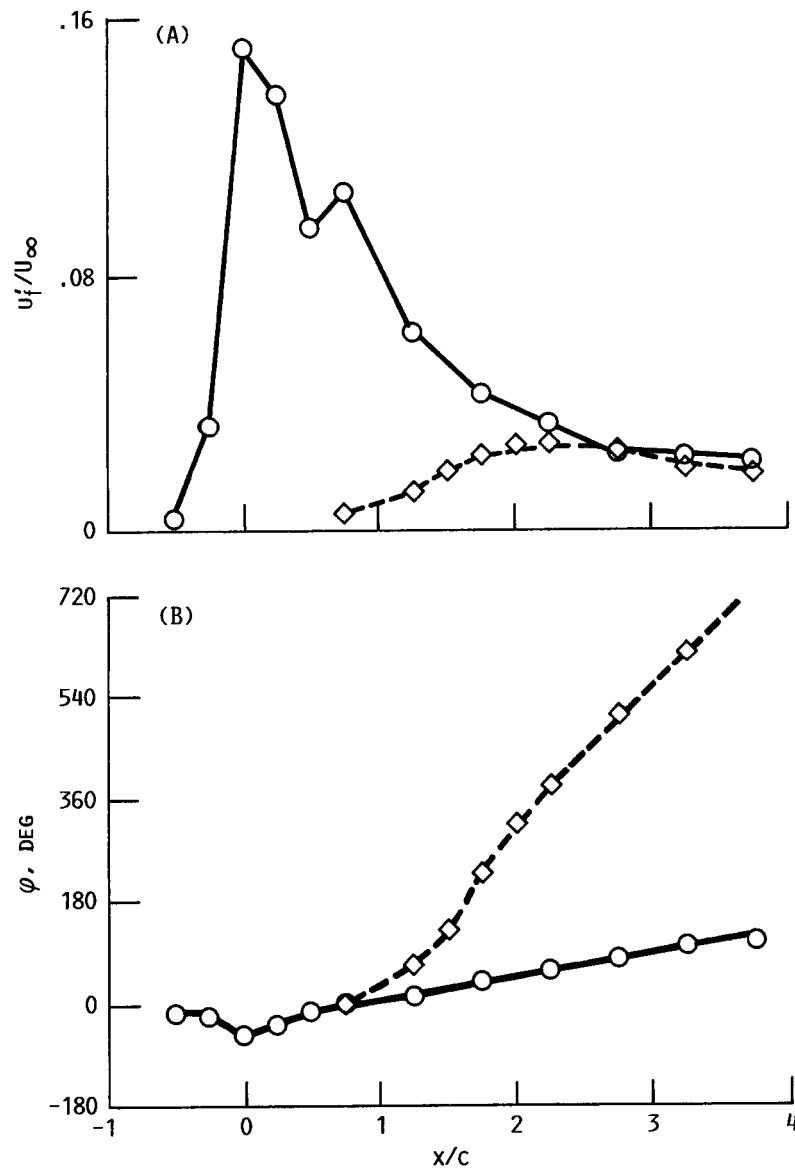


FIGURE 5. - (A) VARIATION OF FUNDAMENTAL (BAND PASSED,  $\Delta f = 0.25$  Hz) RMS VELOCITY FLUCTUATION WITH  $x$ , ALONG  $y/c = 0.1$  AND  $z = 0$ . SOLID CURVE, 7.5-Hz FLUCTUATION AT  $\alpha = 15^\circ$ ; DASHED CURVE, 49-Hz FLUCTUATION AT  $\alpha = 22.5^\circ$ .  $R_c = 10^5$ ;  $u'_\infty/U_\infty = 0.4$  %.

(B) PHASE VARIATION CORRESPONDING TO THE DATA OF (A).

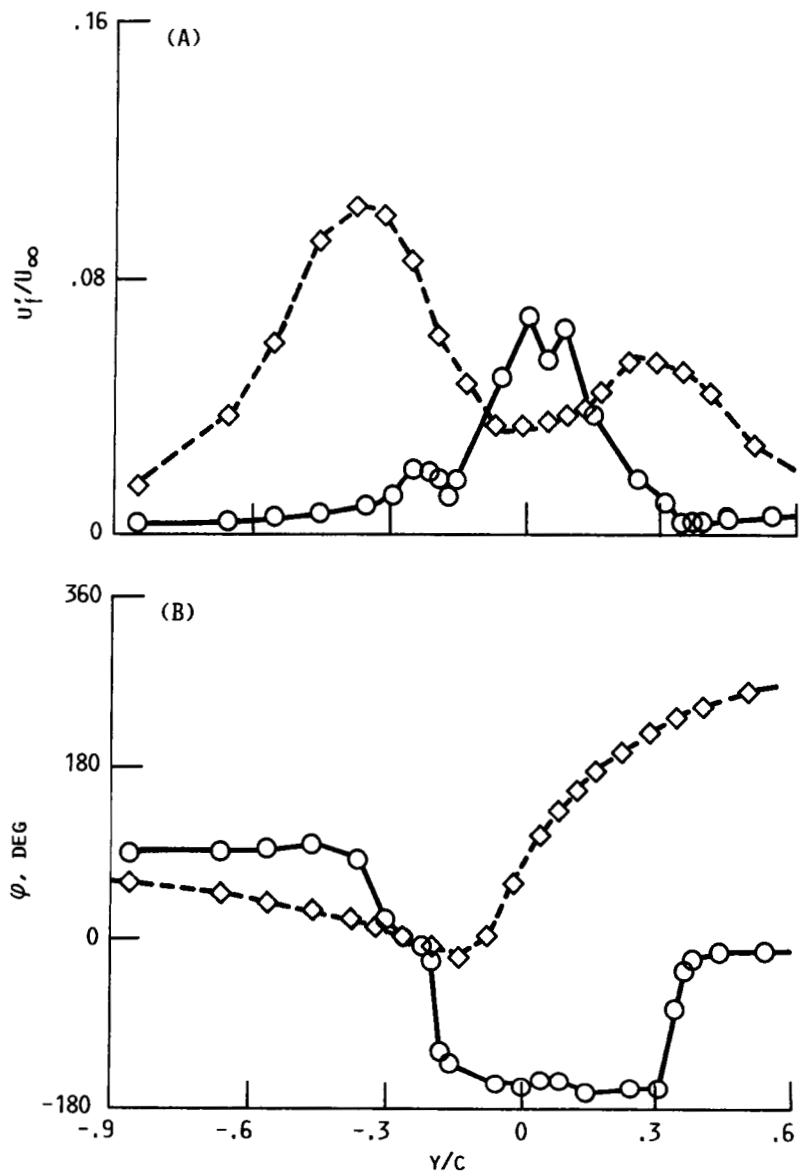


FIGURE 6. - (A)  $u_i'/U_\infty$  VERSUS  $y/c$  MEASURED AT  $z = 0$  AND  $x/c = 1.75$  FOR THE TWO CASES OF FIGURE 5. (B) CORRESPONDING PHASE VARIATION.

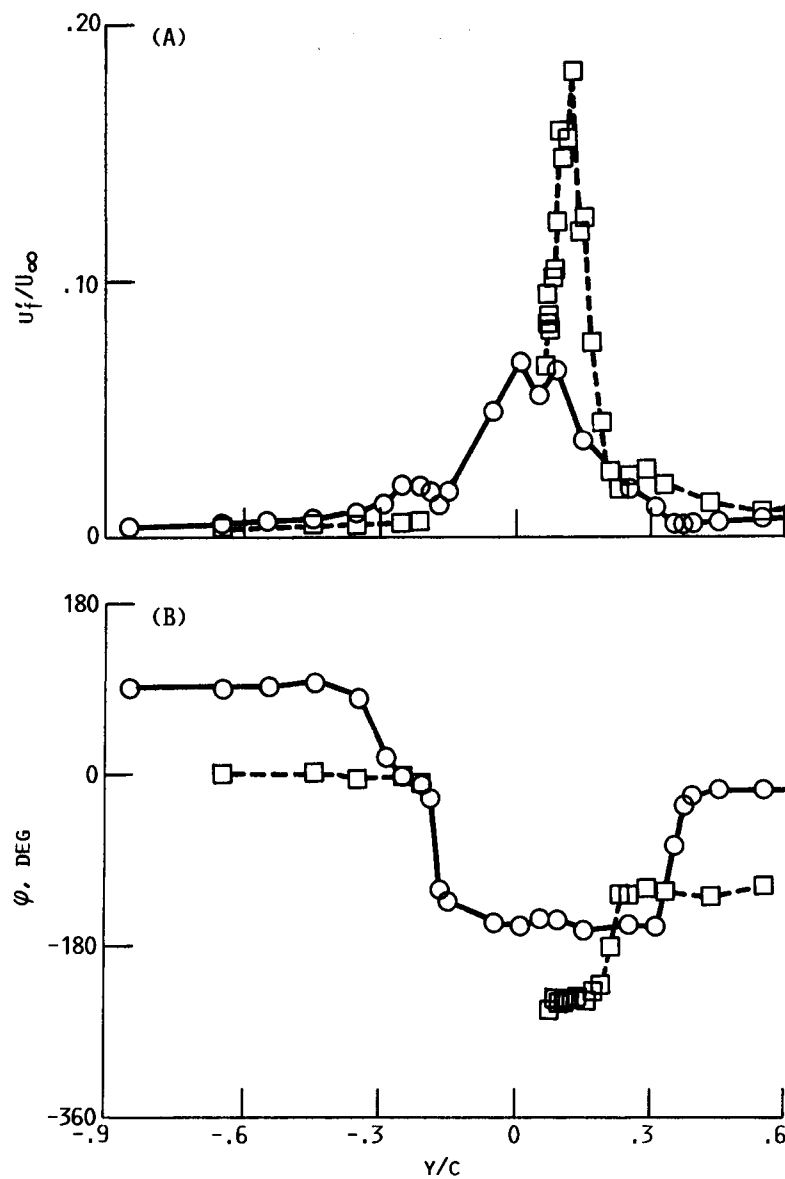


FIGURE 7. - (A)  $u_f'/U_\infty$  VERSUS  $y/c$  FOR  $\alpha = 15^\circ$  CASE. DASHED LINE, MEASUREMENT AT  $x/c = 0.15$  (I.E., AT 0.4  $c$  FROM LEADING EDGE); SOLID LINE, REPLOTED FROM FIGURE 6(A). (B) CORRESPONDING PHASE VARIATION.

ORIGINAL PAGE IS  
OF POOR QUALITY

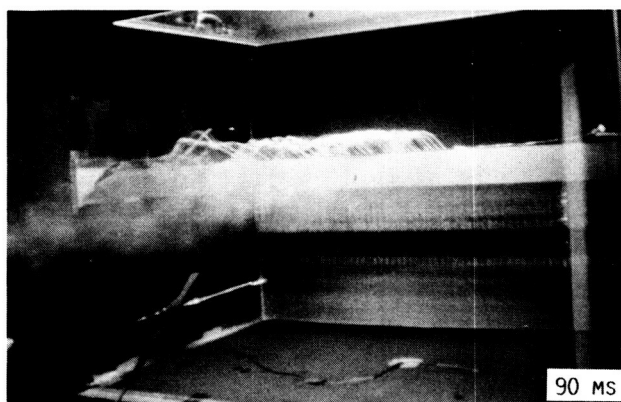
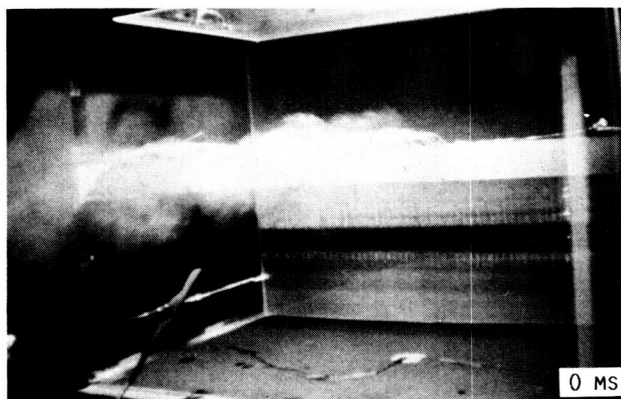


FIGURE 8. - FLOW VISUALIZATION PICTURES (FROM  
MOVIE SEQUENCE) USING HORIZONTAL SMOKE WIRE  
FOR  $\alpha = 15^\circ$  CASE.  $R_C = 7.5 \times 10^4$  YIELDING  
AN OSCILLATION AT 5.5 Hz. SMOKE WIRE AP-  
PROXIMATELY 5 cm UPSTREAM OF LEADING EDGE.

ORIGINAL PAGE IS  
OF POOR QUALITY

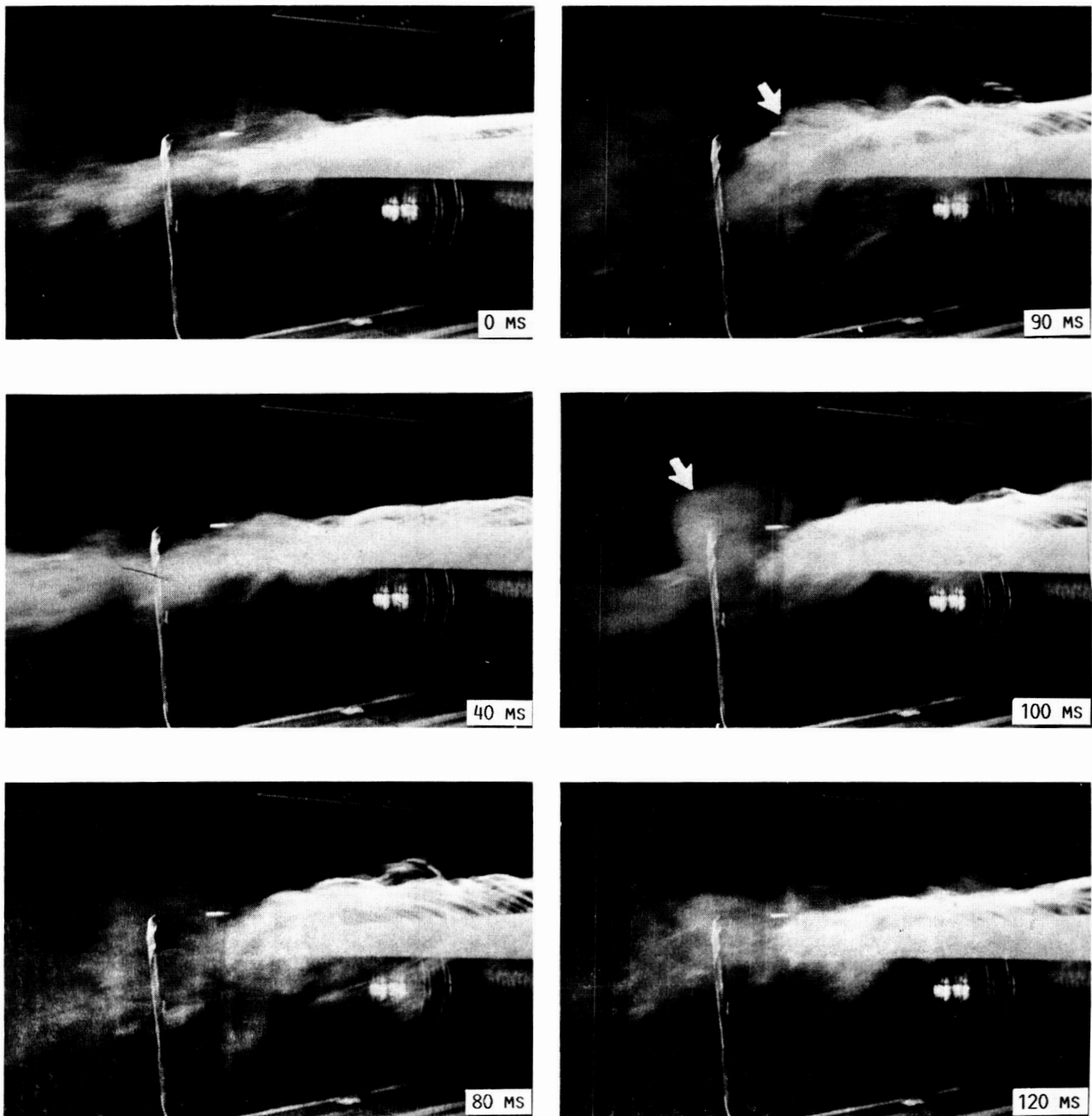


FIGURE 9. - FLOW VISUALIZATION PICTURES FOR SAME FLOW AS IN FIGURE 8 FROM DIFFERENT CAMERA ANGLE.

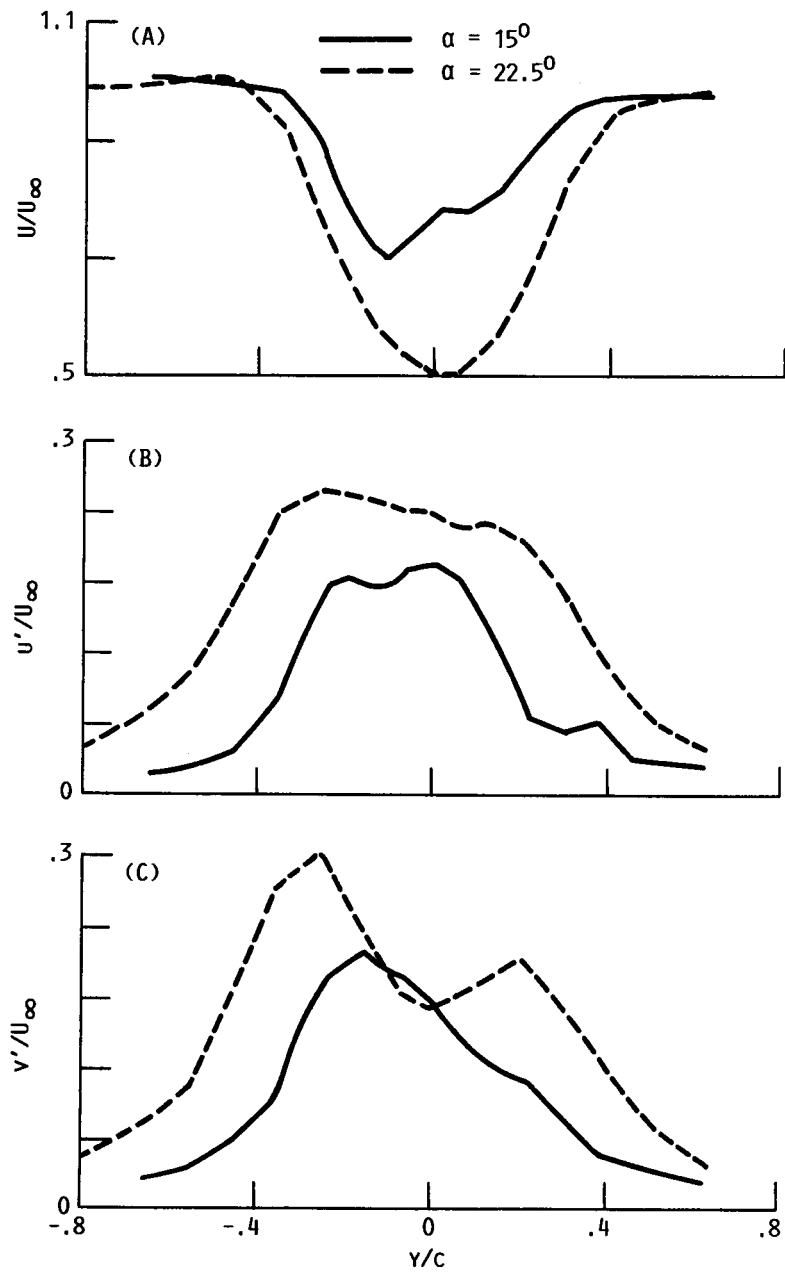


FIGURE 10. - (A) LONGITUDINAL MEAN VELOCITY PROFILES AT  $x/c = 1.75$  AND  $z = 0$ ,  $R_c = 10^5$  AND  $u'_\infty/U_\infty = 0.4\%$ . (B) CORRESPONDING LONGITUDINAL TURBULENCE INTENSITY PROFILES. (C) TRANSVERSE TURBULENCE INTENSITY PROFILES.

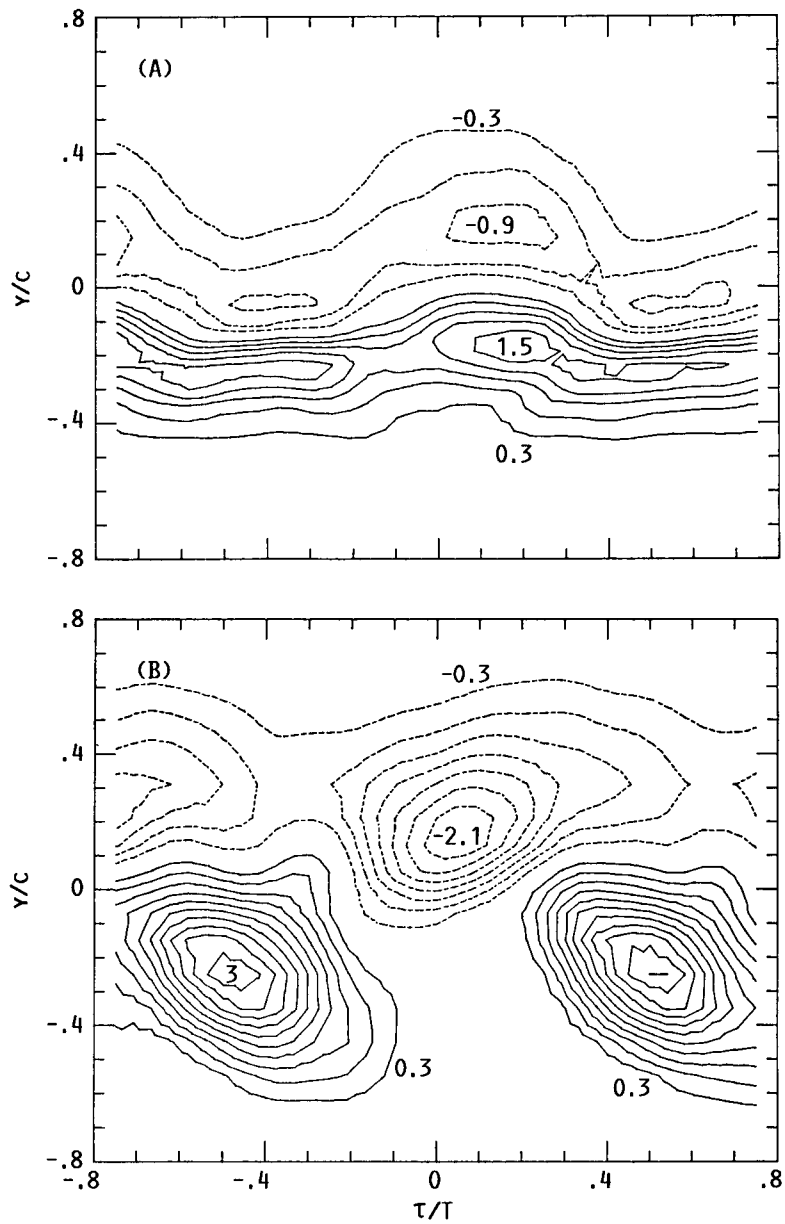


FIGURE 11. - CONDITIONALLY AVERAGED SPANWISE VORTICITY ( $\omega_z$ ) DISTRIBUTION MEASURED AT  $x/c = 1.75$  AND  $z = 0$ .  $\omega_z$  IS NONDIMENSIONALIZED BY  $c/U_\infty$ .  $R_c = 10^5$  AND  $U_\infty'/U_\infty = 0.4\%$ . (A)  $\alpha = 15^\circ$  YIELDING 7.5-Hz OSCILLATION. (B)  $\alpha = 22.5^\circ$  YIELDING 49-Hz OSCILLATION. ABSCISSA (TIME) IS NORMALIZED BY RESPECTIVE PERIODS. CONTOUR LEVELS ARE AT INCREMENTS OF 0.3.

1. Report No. <b>NASA TM-100213 AIAA-88-0131</b>		2. Government Accession No.		3. Recipient's Catalog No.	
4. Title and Subtitle <b>A Natural Low Frequency Oscillation in the Wake of an Airfoil Near Stalling Conditions</b>				5. Report Date	
				6. Performing Organization Code	
7. Author(s) <b>K.B.M.Q. Zaman and D.J. McKinzie</b>				8. Performing Organization Report No. <b>E-3822</b>	
				10. Work Unit No. <b>505-62-21</b>	
9. Performing Organization Name and Address <b>National Aeronautics and Space Administration Lewis Research Center Cleveland, Ohio 44135-3191</b>				11. Contract or Grant No.	
				13. Type of Report and Period Covered <b>Technical Memorandum</b>	
12. Sponsoring Agency Name and Address <b>National Aeronautics and Space Administration Washington, D.C. 20546-0001</b>				14. Sponsoring Agency Code	
15. Supplementary Notes  <b>Prepared for the 26th Aerospace Sciences Meeting, sponsored by the American Institute of Aeronautics and Astronautics, Reno, Nevada, January 11-14, 1988.</b>					
16. Abstract  <b>An unusually low frequency oscillation in the flow over an airfoil was explored experimentally. Wind tunnel measurements were carried out with a two-dimensional airfoil model at a chord Reynolds number of <math>10^5</math>. During deep stall, at <math>\alpha &gt; 16^\circ</math>, the usual "bluff-body shedding" occurred at a Strouhal number, <math>St_s = 0.2</math>. But at the onset of stall around <math>\alpha = 15^\circ</math>, a low frequency periodic oscillation occurred, the corresponding <math>St_s</math> being an order of magnitude lower. The phe- nomenon took place in relatively "unclean" flow when the freestream turbulence was raised to 0.4 percent, but did not in the cleaner flow with turbulence inten- sity of 0.1 percent. It could also be produced by certain high frequency acous- tic excitation. Details of the flow field are compared between a case of low frequency oscillation at <math>\alpha = 15^\circ</math> and a case of bluff-body shedding at <math>\alpha =</math> <math>22.5^\circ</math>. The origin of the low frequency oscillation traces to the upper surface of the airfoil and is seemingly associated with the periodic formation and break- down of a large separation bubble. The intense flow fluctuations impart signifi- cant unsteady forces to the airfoil but diminish rapidly within a distance of one chord from the trailing edge. At the latter downstream location, the periodic concentration of the spanwise component of vorticity is found to be much lower in the low frequency case than that in the bluff body shedding case.</b>					
17. Key Words (Suggested by Author(s)) <b>Airfoil wake Stall flutter Dynamic stall Flow control</b>			18. Distribution Statement <b>Unclassified - Unlimited Subject Category 02</b>		
19. Security Classif. (of this report) <b>Unclassified</b>		20. Security Classif. (of this page) <b>Unclassified</b>		21. No of pages <b>15</b>	
				22. Price* <b>A02</b>	